IEEE Access
Multidisciplinary | Rapid Review | Open Access Journal

Received October 25, 2019, accepted November 12, 2019, date of publication December 4, 2019,
date of current version December 23, 2019.

Digital Object Identifier 10.1109/ACCESS.2019.2955807

Tooth Surface Contact Analysis of Involute Rotate Vector Reducer Based on a Finite Element Linear Programming Method

WEI YANG[1], XIAOLIN TANG[1], AND QI LIANG[2]
[1]State Key Laboratory of Mechanical Transmission, College of Automotive Engineering, Chongqing University, Chongqing 400044, China
[2]State Key Laboratory of Mechanical Transmission, College of Mechanical Engineering, Chongqing University, Chongqing 400044, China

Corresponding author: Wei Yang (slmt053@126.com)

This work was supported in part by Chongqing Natural Science Foundation, under Grant cstc2018jcyjAX0468, in part by the National Natural Science Foundation of China, under Grant 51705044.

ABSTRACT The deformation compatibility relationship of the general contact object under external normal force and the single secondary internal gear pairs of involute RV reducer under a load torque is derived. By transforming the deformation coordination relationship into a linear programming form, a mathematical model for the analysis of the single secondary internal gear pairs with the tooth surface contact of the involute RV reducer is established. An improved simplex method is used to solve the linear programming problem. The calculation results are compared with the ANSYS simulation values from the three aspects of contact tooth pairs, gear tooth load and tooth surface contact force. The results show that the values obtained by the two methods are almost the same on the contact tooth pairs and the tooth load. In terms of tooth surface contact force, the contact area calculated using the finite element linear programming method is slightly smaller than the ANSYS results, but most of the errors are below 12%, indicating that the tooth surface contact conditions obtained using the two calculation methods are consistent. The accuracy and effectiveness of the finite element-linear programming method are thus verified.

INDEX TERMS Dynamic analysis, gear, finite element, contact, involute rotate vector reducer.

I. INTRODUCTION

A. MOTIVATION AND CHALLENGE

The precision reducer is one of the core components of industrial robots. Precision reducers mainly include harmonic reducers and rotate vector (RV) reducers. Compared with harmonic reducers, RV reducers have the advantages of no flexible wheel deformation, high rigidity and stable backlash accuracy [1]–[3]. In advanced high-speed and heavy-duty robots, RV reducers are gradually replacing harmonic reducers, but the cycloidal gear processing and assembly requirements are high. With the increased research on the involute transmission with small tooth number differences and the improvement of manufacturing processes, the performance of involute small tooth number difference planetary reducers has reached that of cycloidal pin gear reducers, which makes the development of involute RV reducers possible [4]–[6]. Compared with cycloidal RV reducers, involute RV reducers have the advantages of convenient gear processing, low material requirements, insensitivity to the center distance, and small contact stress [7], [8].

Researchers often use profile modification techniques to improve the performance of RV reducers, but the tooth backlash generated after profile modification directly affects the contact condition of the gear pair, which has a significant influence on the transmission performance of RV reducers. However, Transmission clearance is an important index that affects transmission performance of reducer. By using the finite element analysis method, the transmission clearance is adjusted manually, and the quantitative mapping relationship between transmission clearance and transmission performance cannot be established accurately. The finite element-linear programming methods can be used to deal with the problem., the transmission clearance is a design variable, which can not only accurately establish the quantitative mapping relationship between transmission clearance and transmission performance, but also give the optimal value of transmission clearance under the condition of given optimization objective function.

The associate editor coordinating the review of this manuscript and approving it for publication was Ali Zemouche.

B. LITERATURE REVIEW

Yang [9] deduced the calculation formula of the normal clearance value of any tooth pair by unifying the instantaneous position of each tooth pair, and provided a clearance diagram. Under the premise that the stiffness of each tooth pair is the same, the number of the actual meshing teeth with a two-dimensional small tooth number difference and the normal load of each tooth pair were derived, and experimental verification was carried out using a photoelastic and a strain experiment. Shu [10] carried out regression analysis on multiple sets of models obtained through the orthogonal design method, and obtained an empirical formula of the flexibility coefficient of tooth bending deformation. Based on the comprehensive consideration of the elastic deformation and manufacturing error of the gear teeth, the mathematical model of two-dimensional small tooth number difference contact was derived. Zhu *et al.* [11]–[13] performed multiple regression analysis on the base pitch deviation, tooth profile deviation and tooth pitch deviation, which significantly influence the tooth profile clearance. It is considered that the base pitch deviation is the main factor which affects the meshing clearance of small tooth number difference, and the contact tooth number and load distribution of the SHQ40 offset three-ring reducer were calculated using a two-dimensional small tooth number difference contact mathematical model considering elastic deformation, tooth side clearance and manufacturing error. Lu and Ye [14] deduced the mechanical equations of contact problems through the principle of virtual work, and used a set of algebraic equations to represent the constraints, thus obtaining a set of nonlinear algebraic equations describing mechanical equilibrium and constraints. The contact condition and stress distribution of planetary gears with small tooth number difference were analyzed using these equations. Song *et al.* [15] analyzed the operation and stress characteristics of the three-ring reducer. According to the bearing force characteristics, a bearing unit with equivalent stiffness was used to restrain the bearing hole. The internal gear plate finite element model was established in ANSYS, and an elastic dynamic model of the ring reducer considering the bending deformation, meshing stiffness, bearing stiffness and eccentric sleeve error of the input and support shafts was derived. The finite element analysis and the elastic dynamics model of the ring reducer were used to calculate the force of each component in the reducer. Based on linear programming method that was proposed by Conry, Li derived the mathematical model of the small tooth number difference transmission contact problem under the condition of internal gear pair mesh, taking into account the pin and bearing effects [16], [17]. The compliance matrix and the initial clearance were obtained using the finite element method. The finite element-linear programming method was used to calculate the number of the contact tooth pairs of the small tooth number difference gear pairs, the tooth surface load distribution, the pin shaft and the bearing ball force. Liu *et al.* [18] used the finite element method to analyze the change of the tooth surface contact state, contact pressure and sliding distance with time in the whole process of NN-type small tooth number difference reducer from mesh in to mesh out. Huang *et al.* [19] established a finite element model of a new involute planetary gear reducer using a finite element method, obtained the equivalent stress distribution diagram of the gear pair, and calculated the change curve of the overall stiffness of the internal gear pair with time. Zhang *et al.* [20] integrated gear pairs, bearing elastic deformation and torsional deformation of the shaft, established the deformation coordination conditions of each motion pair of the small tooth number difference reducer, and established an elastic static equation of the planetary gear reducer with small tooth difference using the substructure synthesis method. Huang [21] extended the external meshing single tooth stiffness calculation equation to the internal meshing field, and obtained the equation of the internal meshing single tooth stiffness, considering the main and driven gear stiffness as equivalent to a series spring to obtain internal meshing single tooth stiffness. Liu [22] established a mathematical model of load distribution with a small tooth number difference considering the base pitch error and combined it with a Monte Carlo method to generate the base pitch error randomly. He then analyzed the influence of the base pitch error on the mesh of the gears with small tooth number difference. Zhou *et al.* [23] established a force-coupling mode for the involute 2K-V reducer considering sliding friction in ABAQUS.

C. ORIGINAL CONTRIBUTIONS

There are three original contributions that clearly distinguish this research from the aforementioned studies:

1) The deformation coordination relationship of the two-stage internal gear pair of the involute RV reducer under a load torque under the premise of linear elasticity is derived. By transforming the deformation coordination relationship into a linear programming form, a mathematical model for studying the contact problem of the two-stage internal gear pair is obtained.

2) Combined the graphing method and the two-dimensional calculation method of the number of internal meshing teeth of small tooth number difference, and concluded that the contact area of the single secondary internal gear pairs reduces the calculation scale of compliance matrix and linear programming problem.

3)The differences between the finite element-linear programming method and the ANSYS simulation are compared from the aspects of contact tooth pairs, gear tooth load and tooth surface contact force, and the accuracy and effectiveness of the proposed finite element linear programming method are verified.

D. OUTLINE OF THIS PAPER

The rest of the paper is organized as follows. The mathematical model of two-stage internal meshing contact of involute RV reducer is introduced in section II. How to determine the contact area in section III. The calculation method

of compliance matrix and initial clearance is described in section IV. Calculation and simulation of two-stage internal mesh contact force of involute RV reducer are performed in section V. Finally, conclusions are summarized in Section VI.

II. MATHEMATICAL MODEL OF TWO-STAGE INTERNAL MESHING CONTACT OF INVOLUTE RV REDUCER

Li [16] and Liu and Yu [24] extended the finite element linear programming method to deal with the tooth surface contact problem based on the work of CONRY [17]. All potential contact points on the gear pair contact surface satisfy the deformation coordination relationship shown in Equations (1) and (2):

$$\sum_{j=1}^{n}(\chi_{kj}+\chi_{k'j'})F_j+\varepsilon_k-\delta-Y_k=0 \tag{1}$$

where n is the total number of contact points, χ_{kj} and $\chi_{k'j'}$ are the compliance coefficients, F_j is the $j-j$' point normal force, ε_k is the initial clearance, δ is the rigid displacement, and Y_k is the slack variable.

$$\sum_{j=1}^{n}F_j=P \tag{2}$$

where P is the external load.

By adding artificial variables and formulating objective functions, the problem is formulated as a linear programming problem to find the optimal value [16], [17], [24], as shown below:

$$\min U=\{C\}\{U\} \tag{3}$$

where U is objective function.

$$\begin{aligned}
\text{s.t.}\ &-[S]\{F\}+\delta\{e\}+[I]\{Y\}+[I]\left\{\overline{U}\right\}=\{\varepsilon\}\\
&\{e\}^{\mathrm{T}}\{F\}+U_{n+n+1}=P\\
&F_k\geq 0,\quad Y_k\geq 0,\ \delta\geq 0,\ \varepsilon_k\geq 0(k=1,2,\cdots,n)\\
&U_{n+l}\geq 0(l=1,2,\cdots,n+1)\\
&Y_k=0\ \text{or}\ F_k=0
\end{aligned} \tag{4}$$

where $\{C\}=(1)_{1\times(n+1)}$ is a $(n+1)$-dimensional row vector, $\{F\}=[F_1,F_2,\cdots,F_n]^{\mathrm{T}}$, $\{\varepsilon\}=[\varepsilon_1,\varepsilon_2,\cdots,\varepsilon_n]^{\mathrm{T}}$, $\{U\}=[U_{n+1},U_{n+2},\cdots,U_{n+n+1}]^{\mathrm{T}}$, $[S]=\left(S_{ij}\right)_{n\times n}=\left(\chi_{ij}+\chi_{i'j'}\right)_{n\times n}\ i=1,2,\cdots,nj=1,2,\cdots,n$. $\{e\}=(1)_{n\times 1}$ is a n-dimensional column vector, and $[I]$ is the identity matrix. Here, $\left\{\overline{U}\right\}=[U_{n+1},U_{n+2},\cdots,U_{n+n}]^{\mathrm{T}}$, $\{Y\}=[Y_1,Y_2,\cdots,Y_n]^{\mathrm{T}}$.

The working principle of the involute RV reducer is the same as that of the common cycloidal pin RV reducer, except that the two-stage cycloidal pinwheel drive is replaced by an involute internal meshing gear pair. The Schematic diagram of transmission is shown in Fig. 1. Internal gear 6 is fixed to the frame, and the output disk transmits power. During operation, the motor drives input shaft 1 to rotate, thereby driving input gear shaft 2, which is fixed to the input shaft. Input gear shaft 2 drives the rotation of planetary gear 3 through external

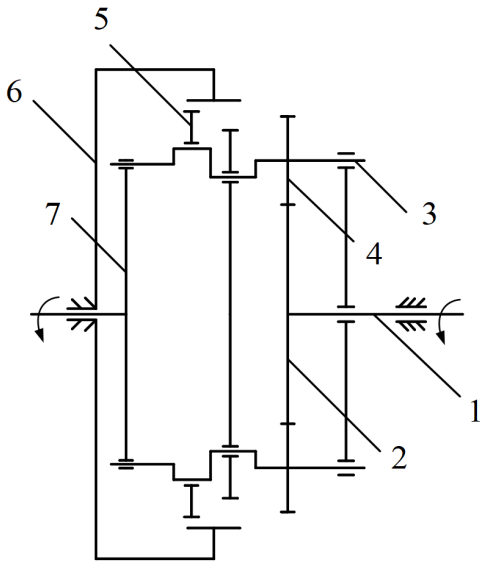

FIGURE 1. Schematic diagram of Involute RV reducer transmission.1-input shaft 2- input gear shaft 3- planet gear 4-crank shaft 5-external gear 6- internal gear 7- output disk.

mesh. Crankshaft 4 is fixed to planetary gear 3 and is moved to external gear 5 through the bearing output to perform a co-rotating motion about the axis of the input shaft. Internal gear 6 causes the external gear to rotate in the reverse direction through the internal meshing action with external gear 5, and outputs the rotation motion to output disk 7 using crankshaft 4 as a medium.

Since the two external gears have the same structural dimensions and we ignore manufacturing and assembly errors and the influence of the elastic deformation of the support on the meshing of the gear pair, it can be assumed that the meshing state of the two external gears and the internal gear are exactly the same, and respectively bear half of the output torque [25]. Therefore, if the friction between the contact faces is ignored, it is only necessary to perform single-pair two-stage internal gear pair contact analysis.

For the two-stage internal gear pair of the RV reducer, the contact teeth will deform elastically under the load torque, and the external gear will rotate about its center by an additional angle [25]–[27]. Since the initial clearance between the internal gear pairs is small, the displacement caused by the elastic deformation will cancel the smaller initial clearance, causing the original non-contact teeth to enter the mesh, resulting in a multi-tooth meshing effect.

Moreover, since the internal and external gear tooth profiles have a similar radius of curvature and are in the same direction, the gear contact area becomes large, and the line contact becomes surface contact. Therefore, the direction of the contact force of different teeth is different, and the direction of the force between the contact points of different positions of the same tooth is also different, as shown in Fig. 3.

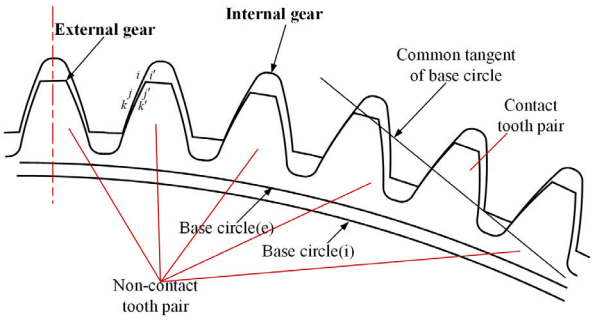

FIGURE 2. Involute multi-teeth internal meshing with small tooth number difference. (e)-external gear (i)-internal gear.

Since the gear contact deformation is small, the shape of the tooth profile after deformation is still an ideal involute. According to the involute tooth profile property, the direction of the contact point force is tangent to the base circle, so the relation of the sum of potential contact points of the two-stage internal meshing gear pair can be obtained similarly to equation (3):

$$\sum_{i=1}^{n} F_i = {}^{T}/_{r_{b1}} \tag{5}$$

where T is the load torque experienced by a single external gear in the internal gear pair, while r_{b1} is the base circle radius of the external gear.

It is assumed that the contact pair *i*-*i'* in Fig. 2 is in contact under the action of the additional corner θ, and the point $i(i')$ is elastically deformed in the normal direction of the contact point by $\omega_i(\omega_{i'})$. Then, the sum of the total elastic deformation amount $(\omega_i + \omega_{i'})$ between the contact points and the initial normal clearance ε_i between the contact points is equal to the displacement δ_i of the i-th point in the direction of the contact force. For the non-contact point, the sum of the normal elastic deformation amount ω_i and the initial ε_i normal clearance between the contact points should be smaller than the displacement δ_i of the i-th point in the direction of the contact force.

$$\omega_i + \omega_{i'} + \varepsilon_i - \delta_i \geq 0 \tag{6}$$

where $i = 1, 2, \cdots, n$.

The displacement of the i-th point in the direction of the contact force δ_i is [28]:

$$\delta_i = r_{ci}\theta \ \cos \ \alpha_i = r_{b1}\theta \tag{7}$$

where r_{ci} is the radius of the contact point i on the external gear tooth profile, θ is the additional corner arc value of the external gear rotation, and α_i is the external gear's i-th point pressure angle.

The slack variable Y_i is introduced, and equation (7) is substituted into equation (6). The deformation amount is expressed by the sum of the flexibility coefficient and the force product, and equation (6) can be converted into:

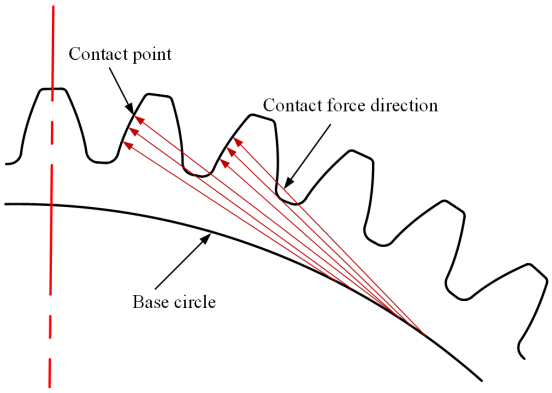

FIGURE 3. Internal gear contact force.

$$\sum_{j=1}^{n} (\chi_{ij} + \chi_{i'j'})F_j + \varepsilon_i - r_{b1}\theta - Y_i = 0 \tag{8}$$

Equation (8) is the same as Equation (1), as are Equation (5) and Equation (2), so the same linear programming approach can be used.

III. DETERMINATION OF THE CONTACT AREA

A. TWO-DIMENSIONAL SMALL TOOTH NUMBER DIFFERENCE INTERNAL MESHING CONTACT MATHEMATICAL MODEL

When finite element-linear programming is used to deal with the tooth surface contact problem, the number of teeth that are in contact is not known beforehand. If the overall model of the gear pair is established, a large amount of time will be required when the number of teeth is large. To shorten the calculation time of the compliance matrix and improve the solution efficiency, the contact area of the two-stage internal gear pair is preliminarily determined through the graphing method and the two-dimensional calculation method of the number of internal meshing teeth with small tooth number difference. The two-dimensional calculation model of the number of internal meshing teeth with small tooth number difference derived from [29], [30] is as follows:

$$\begin{bmatrix} \frac{1}{k_0} & \frac{1}{k_1} & 1 & \cdots & 1 \\ & -\frac{1}{k_1} & & & \\ & \frac{1}{k_1} & -\frac{1}{k_2} & & \\ & & \ddots & \ddots & \\ & & & \frac{1}{k_{n-1}} & \frac{1}{k_n} \end{bmatrix} \begin{bmatrix} \overline{F}_0 \\ \overline{F}_1 \\ \overline{F}_2 \\ \vdots \\ \overline{F}_n \end{bmatrix} = \begin{bmatrix} T/r_b \\ Br_b(\varphi_1 - \varphi_0) \\ Br_b(\varphi_2 - \varphi_1) \\ \vdots \\ Br_b(\varphi_n - \varphi_{n-1}) \end{bmatrix} \tag{9}$$

TABLE 1. Main parameters of two-stage internal gear pair and machining tool.

	internal gear	external gear
Tooth number	240	236
Module(mm)	0.58	0.58
Pressure angle(°)	20	20
Addendum coefficient	1	0.6328
Modification coefficient	0.55028	-0.4
Tooth width(mm)	14	6.5
Center distance(mm)	1.5	1.5
Tool radius(mm)	0.116	0.116

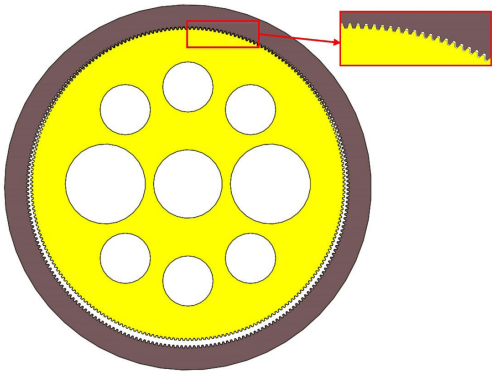

FIGURE 4. Single two-stage internal gear pair.

Since the number of meshing pairs is unknown, the meshing pairs $n = 1, 2, 3, \cdots$ is taken and substituted in (9), until the maximum meshing number where negative elements do not appear in the solution vector $[\overline{F}_0\ \overline{F}_1\ \overline{F}_2\ \ldots \overline{F}_n\ ]^{\mathrm{T}}$ gives the gear meshing pairs. The gear tooth stiffness is calculated according to equation (10), and the elastic deformation is calculated by the material mechanics method [31], [32].

$$k_i = \frac{\overline{F}_i}{B\overline{\omega}_i} \tag{10}$$

where $\overline{F}_i$ is the contact force of the i-th pair of teeth, k_i is the meshing stiffness of the i-th pair of teeth, and B is the gear meshing width.

After finding the initial contact tooth pair number, the initial clearance angle and the gear meshing stiffness according to the graphing method, the number of the contact teeth can be obtained by substituting these values with the load torque in equation (9).

B. CALCULATION RESULTS

The main parameters of the internal gear of the involute RV reducer and its machining tool studied in this paper are shown in Table 1. The external load makes the single pair of internal gear pairs withstand 100N·m load torque. To facilitate the description of the tooth pairs, the tooth pairs are numbered as shown in Figs. 4 and 5. The starting number 1 is the tooth pair

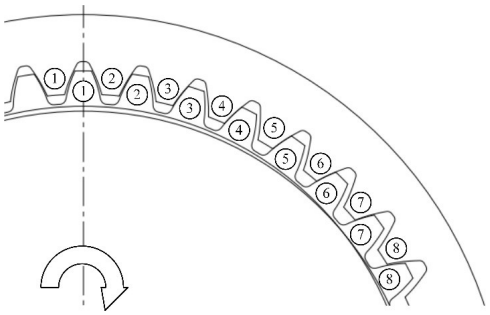

FIGURE 5. Tooth pair number.

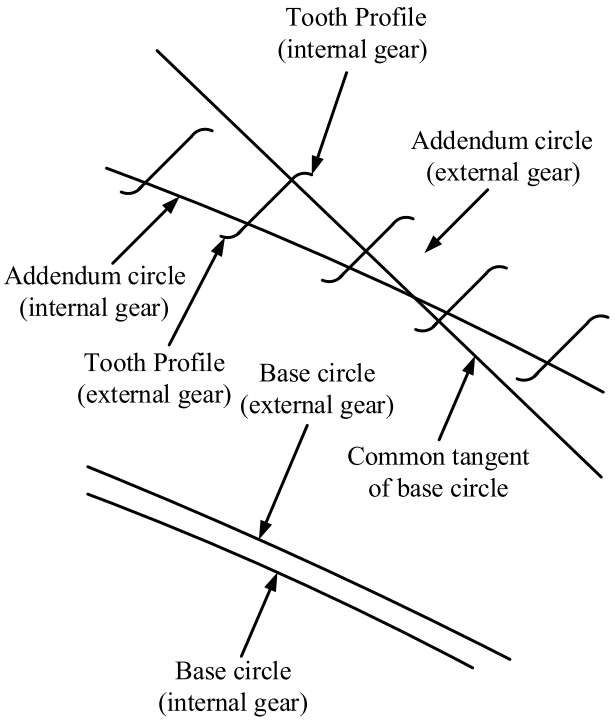

FIGURE 6. Initial contact tooth pair.

TABLE 2. Load of each tooth pair.

Tooth pair number	14	15	16	17	18	19	20
Load (N)	115.1	270.4	338.9	362.9	276.3	183	8.3

on the centerline, and the number increases in a clockwise direction.

To formulate the internal and external gear tooth profile curve and the base circle common tangent in MATLAB, the tooth pair on the actual mesh line is taken as the initial contact tooth pair, as shown in Fig. 6.

7 contact tooth pairs are obtained through the calculation, where the teeth with indices 14-20 are involved in the contact. The load of each tooth pair is shown in Table 2:

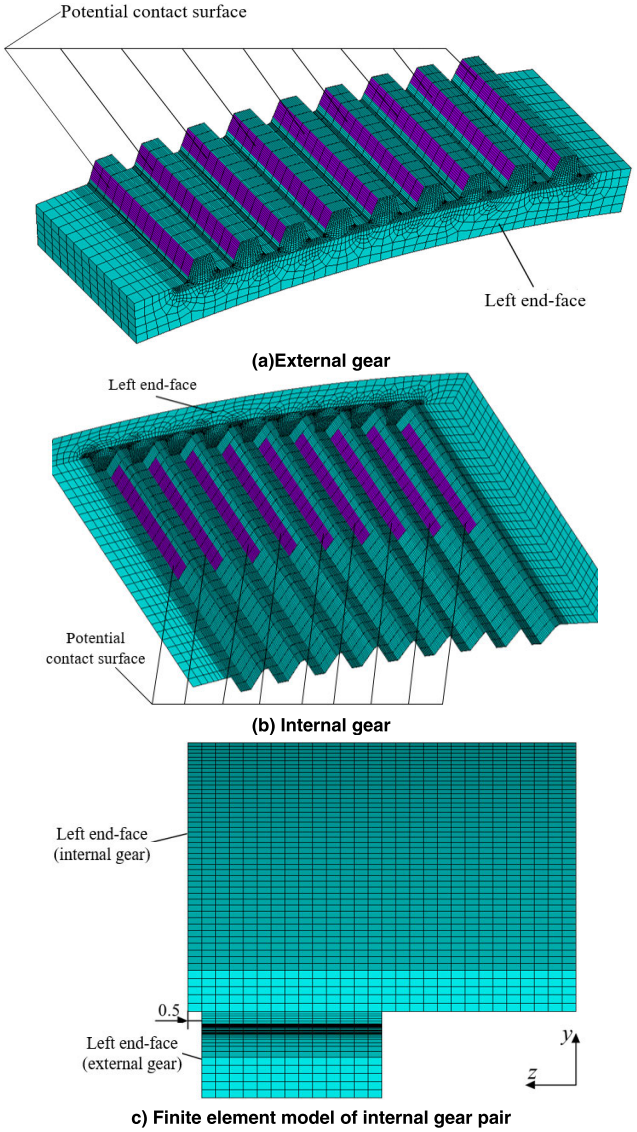

FIGURE 7. Potential contact points.

TABLE 3. Potential contact surface mesh number of segments in the tooth height direction.

Tooth pair number	13	14	15	16	17	18	19	20	21
Number of mesh segments	10	10	10	10	9	9	8	8	8

IV. CALCULATION OF THE COMPLIANCE MATRIX AND DETERMINATION OF INITIAL CLEARANCE

A. CYCLIC LOADING METHOD FOR COMPLIANCE MATRIX OF GEAR PAIRS

The partial finite element model of the two-stage internal gear pair of the involute RV reducer is shown in Fig. 7. The external gear tooth width is divided into 13 segments, while the internal gear tooth width is divided into 28 segments. The number of mesh segments of the potential contact surface in the tooth height direction is shown in Table 3. During operation, the internal gear is fixed, and the external gear rotates through a certain angle in the counterclockwise direction and is subject to elastic deformation. The potential contact surface is shown in Fig. 7, and the contact point is the node on the contact surface. The number of potential contact points on the tooth pair is shown in Table 4, the total of which is 1274.

TABLE 4. Potential contact points of each tooth of internal and external gears.

Tooth pair number	13	14	15	16	17	18	19	20	21
Potential contact points	154	154	154	154	140	140	126	126	126

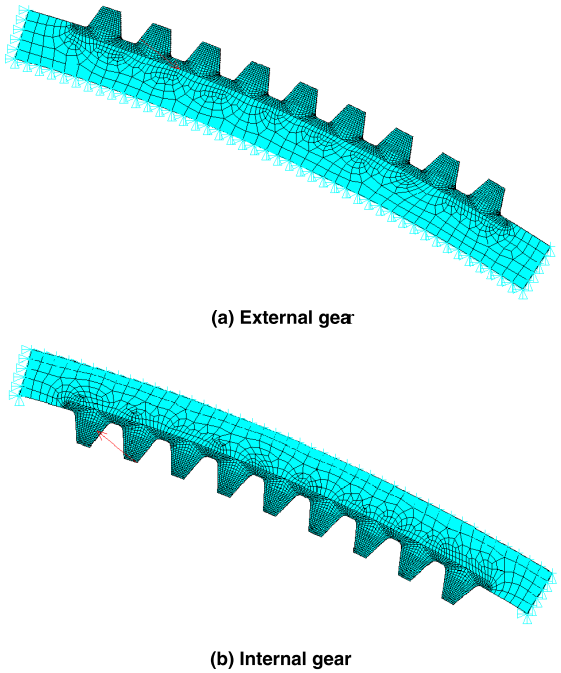

FIGURE 8. Gear compliance matrix calculation model.

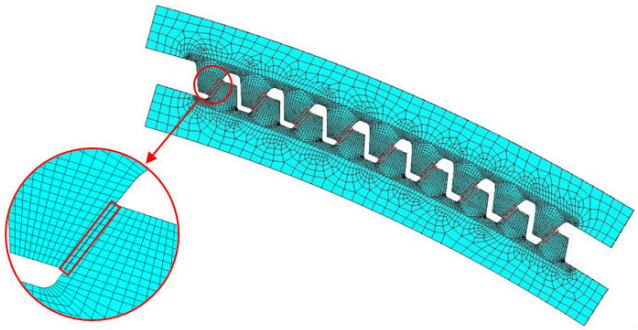

FIGURE 9. Clearance of contact points.

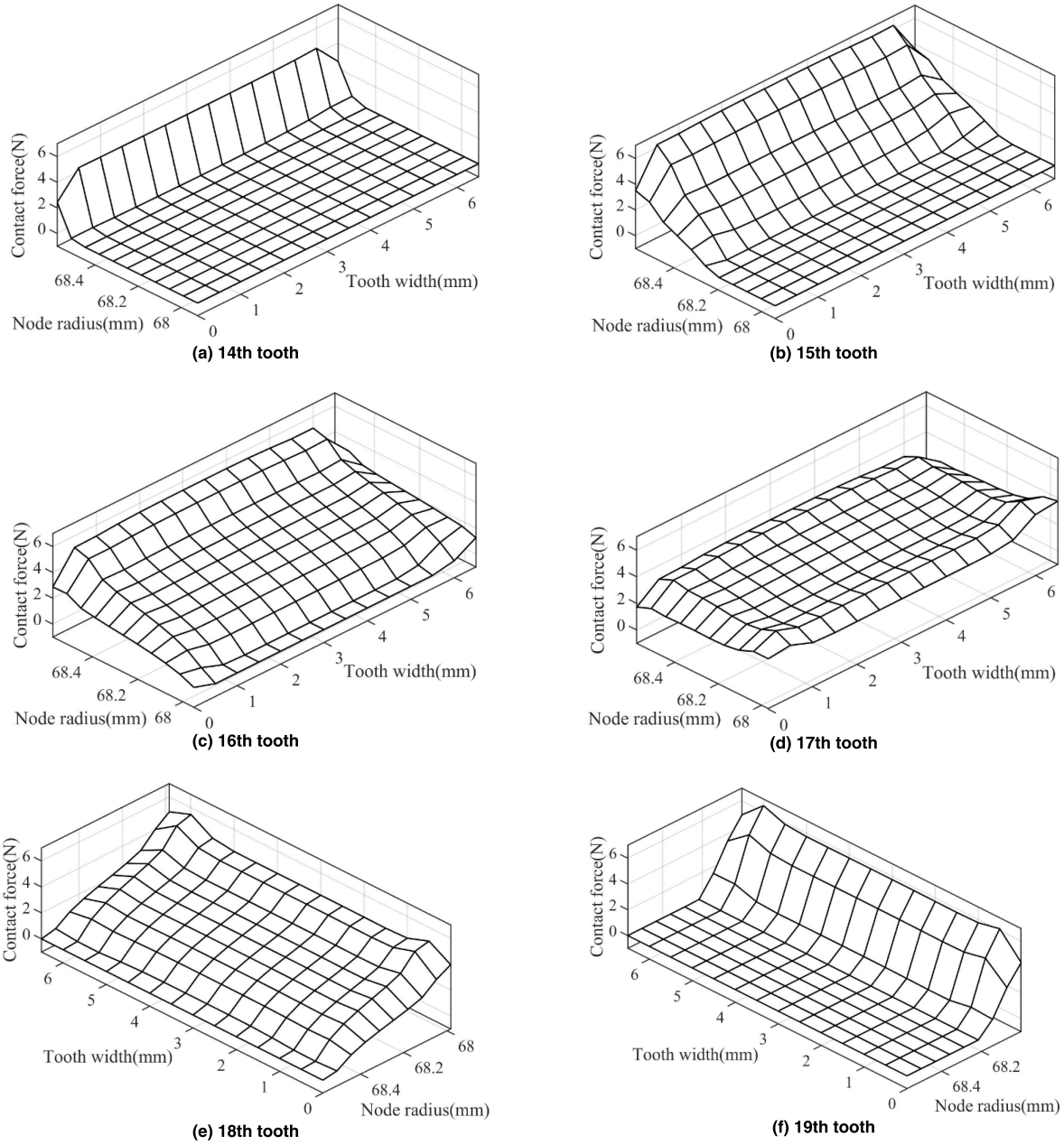

FIGURE 10. External gear tooth surface contact force calculated using the finite element-linear programming method.

When calculating the compliance matrix $[S]$, the internal and external gear boundaries are fixed separately, as shown in Fig. 8. The unit normal force is applied to the potential contact point j of the tooth profile, and the statics solution is performed. The displacements of the 1274 potential contact points in the respective normal directions are respectively obtained, and all the contact points are placed in a column vector in a certain order. Repeating the above operation for all 1274 points, the flexibility coefficient column vector under each unit force is obtained, and all the column vectors are assembled to obtain the internal and external gear flexibility matrices $[\chi']$, and $[\chi]$, with dimensions 1274 $\times$ 1274, respectively. Finally, the two flexibility matrices are added to obtain the gear pair compliance matrix $[S]$.

B. INITIAL CLEARANCE

The x- and y-coordinate values of the nodes were obtained in the global Cartesian coordinate system in ANSYS. The initial distance of potential contact points was calculated, and the initial distance was divided by the radius of the corresponding external gear node. At this time, the initial contact angles of the potential contact points were obtained, and the initial clearance of the internal gear pair was also obtained by multiplying by the radius of the base circle of the gear.

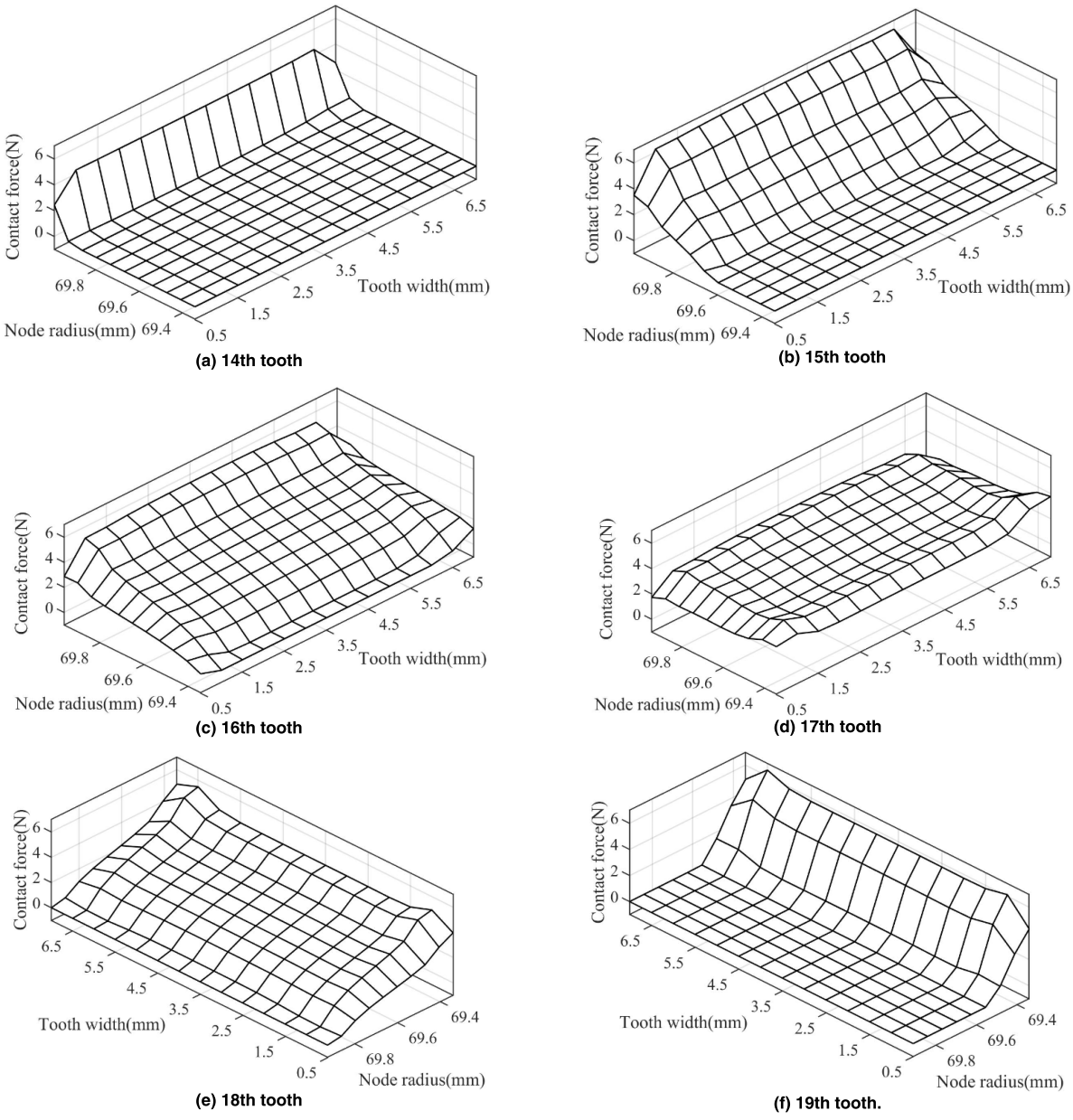

FIGURE 11. Internal gear tooth surface contact force calculated by finite element-linear programming method.

V. CALCULATION AND SIMULATION OF TWO-STAGE INTERNAL MESH CONTACT FORCE OF INVOLUTE RV REDUCER

A. FINITE ELEMENT LINEAR PROGRAMMING METHOD CALCULATION RESULTS

The finite element linear programming method shows that 14-19 teeth are in contact, i.e. a total of 6 pairs, which is one pair less than the number obtained using the two-dimensional contact algorithm. The teeth with indices 13, 20 and 21 are not in contact, and therefore the contact force of the tooth surface is zero. The external gear tooth surface contact force distribution is as shown in Fig. 10, and the tooth width coordinate axis origin is located at the left end surface shown in Fig. 7(c).

In Fig. 10, the 17th tooth is the initial contact tooth, and its load is the largest. Teeth 14-16 the mesh in teeth, and 18 and 19 are the mesh out teeth. The contact force distribution of the tooth surface conforms to the clearance distribution law. The finite element linear programming method considers the force of the same pair of contact points as equal and opposite in the calculation of the contact force. So, the internal gear contact point force is the same as the external gear force in Fig. 10, except that the position on the internal gear is different, as shown in Fig. 11.

The tooth pair load and minimum clearance distribution are shown in Fig. 12. It can be seen that the minimum clearance on the left tooth pairs of the initial contact tooth pair 17 is smaller than the minimum clearance on the right tooth pairs,

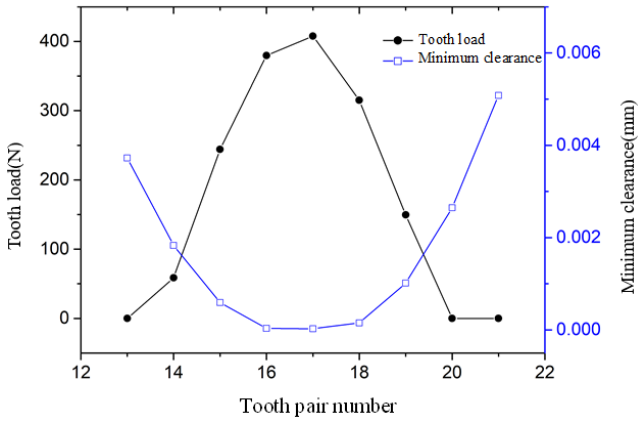

FIGURE 12. Tooth pair load and clearance distribution.

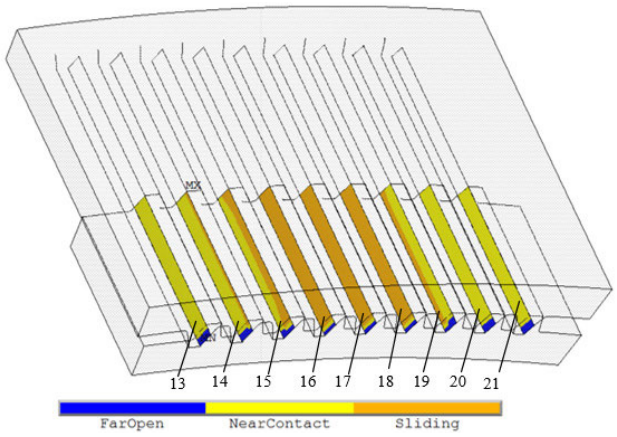

FIGURE 13. Contact teeth calculated by ANSYS simulation.

so the tooth pair is more prone to contact at this meshing position.

B. ANSYS STATIC SIMULATION

The contact algorithm selected the Lagrangian multiplier method and eliminated the initial clearance, and the friction coefficient was set to zero [33]. The internal gear boundary node displacement degrees of freedom were fixed, the external gear was subject to an additional rotation through the establishment of a node in its center of rotation with the MPC184 beam unit and the external gear inner ring node connection, and limited the central node's x, y and z directions of movement and x-y direction of rotation freedom. A counterclockwise load torque was added in the z direction of the outer gear's center node.

In Fig. 13, "Sliding" represents the contact area. The simulation results show that teeth 14-19 participate in the contact, a total of 6 pairs, which is consistent with the finite element linear programming method. The tooth surface contact force distribution on teeth 14-19 is shown in Figs. 14 and 15.

C. COMPARISON OF RESULTS

The finite element linear programming method and the ANSYS simulation both show 6 pairs of contact teeth, namely

TABLE 5. Comparison of external gear tooth load under two calculation methods.

Tooth pair number	13	14	15	16	17	18	19	20	21	Sum
Finite element-linear programming method (N)	--	58.6	244.2	379.7	407.8	315.1	149.5	--	--	1554.9
ANSYS simulation (N)	--	57.5	244.6	381.7	409.0	315.4	149.3	--	--	1557.4
Error	--	1.9%	0.2%	0.5%	0.3%	0.1%	0.1%	--	--	0.2%

TABLE 6. Comparison of internal gear tooth load under two calculation methods.

Tooth pair number	13	14	15	16	17	18	19	20	21	Sum
Finite element-linear programming method (N)	--	58.6	244.2	379.7	407.8	315.1	149.5	--	--	1554.9
ANSYS simulation (N)	--	57.5	244.6	381.7	408.9	315.3	149.3	--	--	1557.3
Error	--	1.9%	0.2%	0.5%	0.3%	0.1%	0.1%	--	--	0.2%

for the tooth pair numbers 14-19. The load on each tooth is shown in Tables 5 and 6 below. "–" indicates that the tooth pair is not in contact. The error percentage in the table is based on the ANSYS simulation values. The calculation equation is shown in (11). From the error data in the table, it can be seen that the two calculation methods are basically consistent in the calculation of the contact pairs and the tooth load distribution.

$$error = |F_{FELPM} - F_{FEM}|/F_{FEM} \tag{11}$$

where F_{FELPM} is the load calculated using the finite element linear programming method and F_{FEM} is the load calculated using ANSYS.

The error of the contact force of the tooth surface was calculated according to (11), and the error values were analyzed statistically to obtain the points which touch on the teeth of 14-19, with a total number 556 points. The horizontal coordinate scale in the error graph is statistically distributed in increments of 10%. The error range indicated by each legend of "Number" is [x, x+10%), that is the starting scale of the error range is a closed interval, and the ending scale an open interval. "Number" indicates the number within the error range, and "Percentage" indicates the ratio of the number within the error range to the total contact point.

As shown in Fig. 16, under the two calculation methods the contact force error value of most external gear tooth surface nodes is small, located in [0%, 10%), accounting for 88.8%. When the error range is expanded to [0%, 20%), the number of errors in this range accounts for 94.4%, while most of the points (24 in total) in [10%, 20%) have an error of 10%-12%. The ratio to the total contact point number is 4.3%, so the

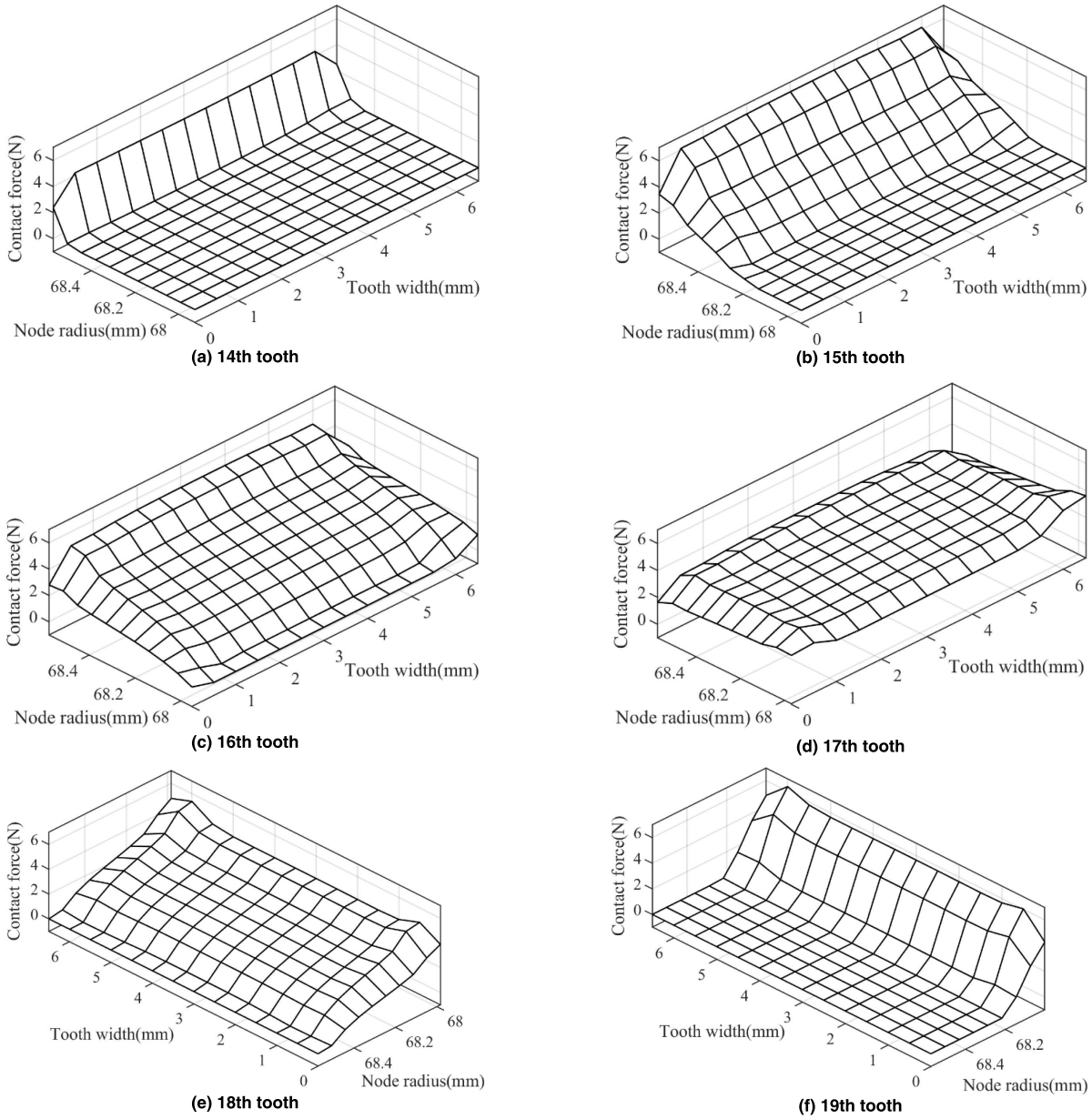

FIGURE 14. External gear tooth surface contact force calculated by ANSYS.

number of points with an error of less than 12% is 93.2%. For points with an error of more than 50%, the contact force at the corresponding contact point is generally small. Table 7 shows the force calculated using ANSYS in 27 contact points with external gear contact point force error above 50% and the maximum contact force ratio on the corresponding gear teeth. The contact point position is represented by the three parameters contained in the brackets. The first parameter represents the tooth pair number, the second represents the contact point tooth width coordinate, and the third represents the radius of the contact point node. It can be concluded from Table 7 that the contact points with larger errors have smaller contact forces, all of which are below 0.23N, and the ratio of the maximum contact force on the corresponding gear teeth is below 3.9%, which has little effect on the analysis of the tooth surface. The 8 points with an error of 100% indicate that the ANSYS simulation results indicate contact at this point, and the finite element linear programming method shows no contact, indicating that the contact area calculated by the finite element linear programming method is slightly smaller than the ANSYS calculation result. Under the two calculation methods, most of the contact point force errors are small. The ratio of larger error point is small and its contact force value is small, which has little effect on the tooth surface analysis. Therefore, it can be considered that the two calculation methods are consistent in determin-

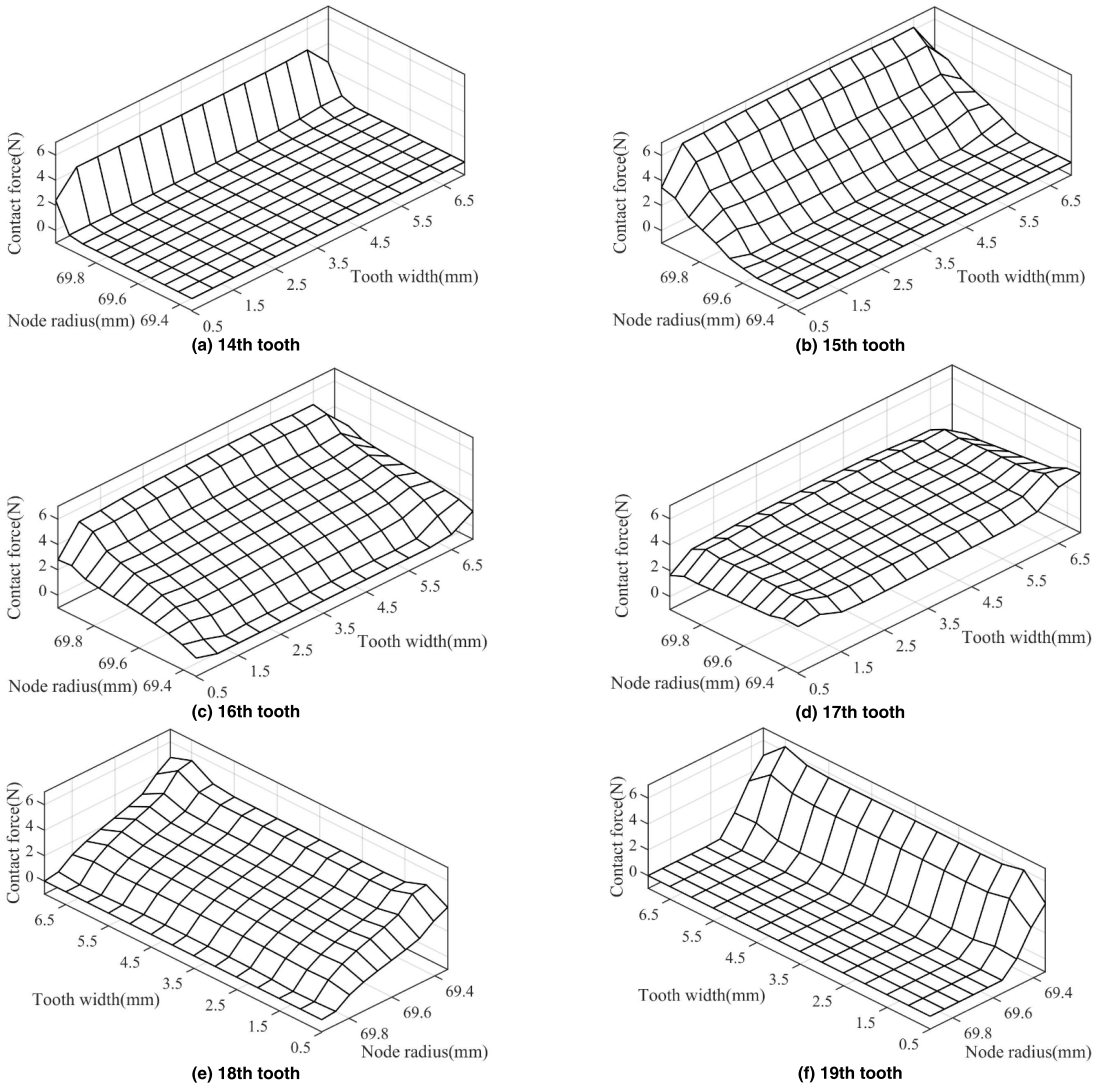

FIGURE 15. Internal gear tooth surface contact force calculated by ANSYS.

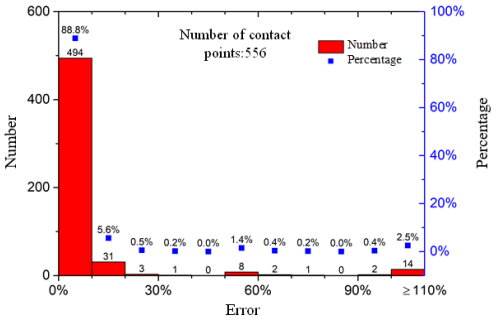

FIGURE 16. External gear tooth surface contact force error statistical chart.

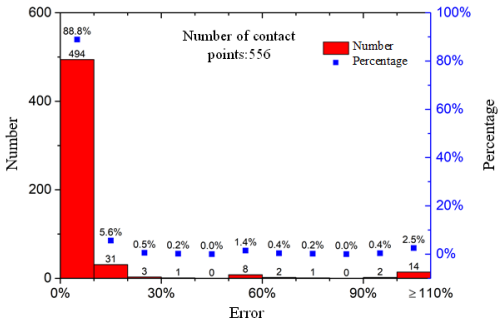

FIGURE 17. Internal gear tooth surface contact force error statistical chart.

ing the contact force distribution of the external gear tooth surface.

The analysis for the distribution of the internal gear tooth surface contact force under the two calculation methods was performed, and the error distribution of Fig. 17 is the same as Fig. 16. The error is 88.8% in the range of [0%, 10%), 93.2% in the range of [0%, 12%], and 94.4% in the range [0%, 20%). The number of error points with an error of more than 50% is 27, accounting for 4.9%. It can be seen from Table 8 that 8 of the larger error points have an error value of 100%, indicating

TABLE 7. ANSYS simulation values of contact points of external gear with more than 50% error.

Coordinate	Error	Contact force(N)	Maximum contact force ratio with gear teeth
(15,0,68.19)	100%	0.224	3.58%
(15,0.5,68.26)	100%	0.002	0.03%
(16,1,68.01)	117%	0.036	0.69%
(16,1.5,68.01)	100%	0.129	2.49%
(16,2,68.01)	100%	0.128	2.47%
(16,2.5,68.01	100%	0.123	2.37%
(16,3,68.01)	100%	0.121	2.33%
(16,3.5,68.01)	100%	0.118	2.27%
(16,4,68.01)	100%	0.118	2.27%
(16,4.5,68.01)	94%	0.108	2.08%
(16,5,68.01)	54%	0.078	1.5%
(16,5.5,68.01)	72%	0.15	2.89%
(16,6,67.95)	52%	0.199	3.84%
(18,0,68.51)	59%	0.104	1.94%
(18,0.5, 68.51)	98%	0.035	0.65%
(18,1, 68.51)	1158%	0.008	0.15%
(18,1.5, 68.51)	101%	0.104	1.94%
(18,2, 68.51)	62%	0.169	3.15%
(18,2.5, 68.51)	55%	0.191	3.56%
(18,3, 68.51)	53%	0.196	3.65%
(18,3.5, 68.51)	53%	0.198	3.69%
(18,4, 68.51)	54%	0.194	3.61%
(18,4.5, 68.51)	62%	0.169	3.15%
(18,5, 68.51)	117%	0.09	1.68%
(18,5.5, 68.51)	141%	0.031	0.58%
(18,6, 68.51)	607%	0.013	0.24%
(19,6.5, 68.22)	58%	0.058	0.91%

TABLE 8. ANSYS simulation value of contact points of internal gear with more than 50% error.

Coordinate	Error	Contact force(N)	Maximum contact force ratio with gear teeth
(15,0.5,69.6)	100%	0.223	3.55%
(15,1,69.66)	100%	0.002	0.03%
(16,1.5,69.4))	117%	0.036	0.69%
(16,2,69.4)	100%	0.129	2.47%
(16,2.5,69.4)	100%	0.127	2.43%
(16,3,69.4)	100%	0.122	2.34%
(16,3.5,69.4)	100%	0.12	2.3%
(16,4,69.4	100%	0.117	2.24%
(16,4.5,69.4)	100%	0.118	2.26%
(16,5,69.4)	95%	0.108	2.07%
(16,5.5,69.4)	55%	0.077	1.48%
(16,6,69.4)	72%	0.149	2.85%
(16,6.5,69.34)	52%	0.198	3.79%
(18,0.5,69.86)	58%	0.106	1.98%
(18,1,69.86)	112%	0.031	0.58%
(18,1.5,69.86)	2965%	0.003	0.06%
(18,2,69.86)	97%	0.108	2.02%
(18,2.5,69.86)	60%	0.173	3.23%
(18,3,69.86)	54%	0.195	3.64%
(18,3.5,69.86)	52%	0.201	3.75%
(18,4,69.86)	52%	0.203	3.79%
(18,4.5,69.86)	53%	0.199	3.72%
(18,5,69.86)	60%	0.174	3.25%
(18,5.5,69.86)	111%	0.094	1.76%
(18,6,69.86)	167%	0.026	0.49%
(18,6.5,69.86)	870%	0.009	0.17%
(19,7,69.56)	58%	0.058	0.91%

that the contact area calculated by the finite element linear programming method is smaller than the ANSYS calculation result. The contact force of the larger error contact point is less than 0.23N, and the ratio of the maximum load of the corresponding gear teeth is less than 3.8%. Similarly, the two calculation methods for the contact force distribution of the internal gear tooth surface are consistent.

In summary, for the three aspects of contact pairs, tooth load distribution and tooth surface contact force distribution, the finite element linear programming method and ANSYS produce almost the same results in the contact tooth pairs and the tooth load distribution. When calculating the contact force of the tooth surface, the contact area calculated by the finite element-linear programming method is slightly smaller than the values calculated using ANSYS. There are a few points with large error value, but the contact force value is smaller, which has less influence on the tooth surface contact analysis. Most of the contact point errors are below 12%. Therefore, the results of the two calculation methods are consistent when analyzing the tooth surface contact conditions, which verifies the accuracy and effectiveness of the finite element linear programming method.

VI. CONCLUSION

In this paper, the finite element-linear programming method is used to deal with the contact problem of the two-stage internal gears of the involute RV reducer. Its principle, method and procedure are introduced. The deformation coordination relationship between contact points of single-pair two-stage internal meshing gear pair is deduced and transformed into a linear programming problem, and finally a mathematical model describing the two-stage internal meshing contact problem of the involute RV reducer is obtained. The improved simplex method is used to calculate the solution and obtain the number of contact teeth, gear tooth load distribution and tooth surface contact force distribution. A finite element simulation model is established in ANSYS, and the finite element linear programming method is compared with the ANSYS simulation values to verify the accuracy and effectiveness of the finite element linear programming method.

Funding: This research was funded by Chongqing Natural Science Foundation, grant number No. cstc2018jcyjAX0468, National Natural Science Foundation of China, grant number No. 51705044.

REFERENCES

[1] X. Huang, W. J. He, and Y. X. Fu, "Overview of industrial robot precision reducer," *Mach. Tool Hydraul.*, vol. 43, no. 13, pp. 1–6, 2015.

[2] X. Tang, W. Yang, X. Hu, and D. Zhang, "A novel simplified model for torsional vibration analysis of a series-parallel hybrid electric vehicle," *Mech. Syst. Signal Process.*, vol. 85, pp. 329–338, Feb. 2017.

[3] W. Yang, X. Tang, and X. Chen, "Nonlinear modelling and transient dynamics analysis of a hoist equipped with a two-stage planetary gear transmission system," *J. Vibroeng.*, vol. 17, no. 6, pp. 2858–2868, 2015.

[4] M. Shuai, M. Shuai, J. Guoguang, G. Jiabei, Z. Ting, and Z. Shengping, "Design principle and modeling method of asymmetric involute internal helical gears," *Proc. Inst. Mech. Eng. C, J. Mech. Eng. Sci.*, vol. 233, no. 1, pp. 244–255, Jan. 2019.

[5] X. Tang, D. Zhang, T. Liu, A. Khajepour, H. Yu, and H. Wang, "Research on the energy control of a dual-motor hybrid vehicle during engine start-stop process," *Energy*, vol. 166, pp. 1181–1193, Jan. 2019.

[6] Y. Qin, C. Wei, X. Tang, N. Zhang, M. Dong, and C. Hu, "A novel nonlinear road profile classification approach for controllable suspension system: Simulation and experimental validation," *Mech. Syst. Signal Process.*, vol. 125, pp. 79–98, Jun. 2019, doi: 10.1016/j.ymssp.2018.07.015.

[7] Z. X. Gong, "A small tooth number difference reducer with partial crankshaft input," *Mech. Des.*, vol. 10, no. 1, pp. 47–50, 1992.

[8] W. Yang and X. Tang, "Modelling and modal analysis of a hoist equipped with two-stage planetary gear transmission system," *Proc. Inst. Mech. Eng., K, J. Multi-Body Dyn.*, vol. 231, no. 4, pp. 739–749, 2017.

[9] X. H. Yang, "Research on the actual contact teeth and bearing capacity of internal gear with small tooth number difference," *Radar Confrontation*, vol. 10, no. 1, pp. 11–19, 1990.

[10] S. Xiao-Long, "Determination of load sharing factor for planetary gearing with small tooth number difference," *Mech. Mach. Theory*, vol. 30, no. 2, pp. 313–321, 1995.

[11] C. C. Zhu, J. Huang, and Q. Wang, "Research on actual contact teeth and load distribution of planetary gear transmission with small tooth number difference," *China Mech. Eng.*, vol. 13, no. 18, pp. 1586–1589, 2002.

[12] X. Tang, X. Hu, W. Yang, and H. S. Yu, "Novel torsional vibration modeling and assessment of a power-split hybrid electric vehicle equipped with a dual-mass flywheel," *IEEE Trans. Veh. Technol.*, vol. 67, no. 3, pp. 1990–2000, Mar. 2018.

[13] W. Yang and X. Tang, "Numerical analysis for heat transfer laws of a wet multi-disk clutch during transient contact," *Int. J. Nonlinear Sci. Numer. Simul.*, vol. 18, nos. 7–8, pp. 599–613, 2017.

[14] Z. H. Lu and Q. T. Ye, "A new mechanical model for elastic contact problems," *Appl. Math. Mech.*, vol. 25, no. 11, pp. 1203–1210, 2004.

[15] Y. M. Song, J. Zhang, and Y. X. Zhang, "Elastic dynamic analysis of ring reducer considering deformation of internal tooth plate," *J. Mech. Eng.*, vol. 42, no. 9, pp. 29–32, 2006.

[16] S. Li, "Contact problem and numeric method of a planetary drive with small teeth number difference," *Mech. Mach. Theory.*, vol. 43, no. 9, pp. 1065–1086, 2008.

[17] T. F. Conry and A. Seireg, "A mathematical programming method for design of elastic bodies in contact," *J. Appl. Mech.*, vol. 38, no. 2, pp. 387–392, 1971.

[18] W. J. Liu, C. S. Song, and Y. Hong, "Meshing impact analysis and modification design of NN type small tooth number difference planetary gear transmission," *China Mech. Eng.*, vol. 23, no. 4, pp. 425–429, 2012.

[19] C. Huang, J.-X. Wang, K. Xiao, M. Li, and J.-Y. Li, "Dynamic characteristics analysis and experimental research on a new type planetary gear apparatus with small tooth number difference," *J. Mech. Sci. Technol.*, vol. 27, no. 5, pp. 1233–1244, 2013.

[20] J. Zhang, S. L. Xie, and P. M. Xu, "Elastic static analysis of a small tooth number difference planetary gear reducer," *J. Agricult. Eng.*, vol. 29, no. 24, pp. 49–55, 2013.

[21] C. Huang, "Dynamic characteristics analysis and nonlinear vibration of planetary gear reducer with small tooth number difference," Ph.D. dissertation, Mech. Des. Theory, Chongqing Univ., Chongqing, China, 2013.

[22] B. B. Liu, "Analysis of tooth load of planetary gears with small tooth number difference under the action of base section error," *Chin. J. Construct. Mach.*, vol. 12, no. 3, pp. 243–247, 2014.

[23] H. J. Zhou, G. W. Zhou, and J. X. Wang, "Structural design and contact simulation of involute 2K-V planetary transmission," *Mech. Transmiss.*, vol. 40, no. 2, pp. 49–53, 2016.

[24] G. Liu and L. Y. Wu, "Three-dimensional contact stress analysis of internal meshing spur gears," *Chin. J. Comput. Mech.*, vol. 11, no. 1, pp. 63–67, 1994.

[25] W. D. He, L. X. Li, and Y. X. Xu, "Force analysis and transmission power of high precision RV transmission," *J. Mech. Eng.*, vol. 32, no. 4, pp. 104–110, 1996.

[26] W. D. He, L. X. Li, and J. Li, "Force analysis of cycloidal gear in RV transmission for robots," *J. Dalian Jiao Tong Univ.*, vol. 20, no. 2, pp. 49–53, 1999.

[27] X. Y. Dong and J. Y. Deng, "Stress analysis of RV transmission mechanism," *J. Shanghai Jiao Tong Univ.*, vol. 30, no. 5, pp. 65–70, 1996.

[28] X. N. Feng, H. Zhang, and S. Y. Ye, "Calculation method of multi-tooth meshing bending strength of internal gears with small tooth number difference," *Mining Mach.*, vol. 37, no. 3, pp. 8–11, 2016.

[29] G. C. Ying, "Research on elastic meshing effect of three-ring transmission," M.S. thesis, Mech. Des. Theory, Tianjin Univ., Tianjin, China, 2004.

[30] X. Tang, L. Zou, W. Yang, Y. Huang, and H. Wang, "Novel mathematical modelling methods of comprehensive mesh stiffness for spur and helical gears," *Appl. Math. Model.*, vol. 64, pp. 524–540, Dec. 2018.

[31] R. W. Cornell, "Compliance and stress sensitivity of spur gear teeth," *J. Mech. Des.*, vol. 103, no. 2, pp. 447–459, 1981.

[32] X. Liang, M. J. Zuo, and T. H. Patel, "Evaluating the time-varying mesh stiffness of a planetary gear set using the potential energy method," *Proc. Inst. Mech. Eng., C, J. Mech. Eng. Sci.*, vol. 228, no. 3, pp. 535–547, 2014.

[33] F. R. Qiao, "Research on gear contact stress and meshing stiffness based on ANSYS," M.S. thesis, Mech. Des. Theory, Dalian Univ. Technol., Dalian, China, 2013.

WEI YANG received the B.S. degree from Northwestern Polytechnical University, Xi'an, China, in 1994, and the M.S. and Ph.D. degrees from Chongqing University, Chongqing, China, in 1997 and 2001, respectively, all in mechanical engineering. Since 2010, he has been a Professor of vehicle engineering with Chongqing University. His research interests include mechanical system dynamics and hybrid drive transmission. He has more than 20 years of research experience in dynamics research field of the transmission, especially in the vibration analysis of the transmission.

XIAOLIN TANG received the B.S. degree in mechanics engineering and the M.S. degree in vehicle engineering from Chongqing University, Chongqing, China, in 2006 and 2009, respectively, the Ph.D. degree in mechanical engineering from Shanghai Jiao Tong University, China, in 2015. From August 2017 to August 2018, he was a Visiting Professor with the Department of Mechanical and Mechatronics Engineering, University of Waterloo, Waterloo, ON, Canada. He is currently an Associate Professor with the State Key Laboratory of Mechanical Transmissions and with the Department of Automotive Engineering, Chongqing University. He is also a committeeman of the Technical Committee on Vehicle Control and Intelligence, Chinese Association of Automation (CAA). He has led and has been involved in more than ten research projects, such as National Natural Science Foundation of China. He has published more than 20 articles. His research focuses on hybrid electric vehicles (HEVs), vehicle dynamics, noise and vibration, and transmission control.

QI LIANG received the B.S. degree in mechanical engineering from the North China University of Water Resources and Electric Power, in 2018. He is currently pursuing the master's degree with Chongqing University. His research interests include vehicle dynamics, noise, and vibration.